



Evaluation of Long-Term Corrosion Fatigue Life of Ship and Offshore Structural Steel

Won Beom Kim^(✉)

Department of Naval Architecture and Ocean Engineering, Ulsan College, Ulsan, Korea
wbkim@uc.ac.kr

Abstract. In this study, an evaluation of the long-term corrosion fatigue life of ships and offshore structural carbon steel was conducted, and the result is compared with data from other experimental studies. The evaluation was carried out as follows:

- 1) First, an evaluation of the increased stress, caused by general corrosion, was conducted to calculate the crack initiation life and propagation life. This stress increase, due to area reduction from the weight loss, was calculated through an evaluation of the corrosion rate obtained from 16 years of published weight loss data from continuous immersion in seawater.
- 2) Second, an evaluation of the moment of crack initiation (N_i), when a crack is initiated at the corrosion pit, was conducted. The depth of the corrosion pit was calculated from 16 years of continuous immersion test data of pit penetration.

To determine the instant of crack initiation at the corrosion pit, the Komai threshold value for crack initiation at the corrosion pits was adopted. To calculate the stress intensity factor of a crack, the Newman-Raju formula was used.

- 3) Finally, the crack propagation life was evaluated from crack initiation to fracture. The results of the evaluation are compared with long-term S-N experimental corrosion fatigue test data.

In this study, the long-term corrosion fatigue life estimation method, using weight loss and pit corrosion data by long-term immersion corrosion data, was investigated. The evaluation results were found to reflect the tendency of long-term S-N fatigue test results.

Keywords: Long-term corrosion fatigue · Corrosion pit · General corrosion · Crack initiation threshold · Fracture mechanics

1 Introduction

Fatigue strength is a key design factor contributing to the strength of ships and offshore structures that must withstand the constant application of loads in the ocean, such as waves, tides, and winds. Additionally, in marine structures such as ships and offshore

structures, corrosion resistance as well as fatigue strength is required. As a countermeasure against corrosion in these structures, corrosion protection is generally obtained by, for example, coating, sacrificial anode, and impressed current cathodic protection. However, corrosion is not always completely prevented, for various reasons, and constantly occurs. The strength of a structure under such corrosive conditions should be fully examined. In this study, a long-term corrosion fatigue life estimation corresponding to the lifetime of a ship or offshore structure was performed. The purpose of this study is to propose a new concept that considers both general corrosion and pitting corrosion in the estimation of the corrosion fatigue life.

2 Background

It is well-known that fatigue, a major structural failure mode, behaves differently in seawater than in the atmosphere.

The phenomenon of corrosion fatigue has been recognized for many years and involves the synergistic effect of corrosion and fatigue, which is more prominent in seawater than in the atmosphere. In ships, corrosion has been dealt with by providing a corrosion margin on the plate. Previous studies have shown that the types of corrosion of certain alloy systems occur in specific forms. That is, general corrosion occurs in mild steel, while pitting corrosion and stress corrosion cracking occur in stainless steel [1].

Meanwhile, it has been established that corrosion pits play an important role in the occurrence of corrosion fatigue crack initiation in hull structural steel [2]. Many papers have also been published that focus on the mechanical characteristics of corrosion pits [3–6]. An important issue regarding corrosion pits is the possibility of a mechanical evaluation of the occurrence of cracks. In previous studies, crack initiation was determined to begin when the crack length reached 1 mm or when the fatigue crack reached the plate thickness size. This judgment is convenient but somewhat ambiguous to the mechanical or physical meaning. In addition, general corrosion was observed with the naked eye, and numerous corrosion pits were observed under an electron microscope in the data [7] of the plate taken from a ship that was in operation for 17 years, as shown in Fig. 1.

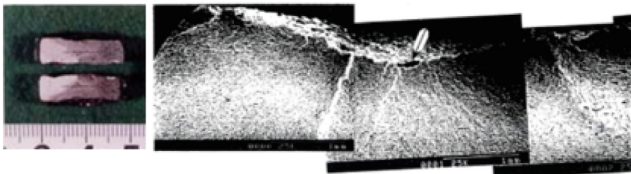


Fig. 1. Fatigue test results of steel plate taken from aged ship and corrosion pit of crack initiation site.

The fatigue test results under atmospheric and seawater conditions confirm that cracks begin from the corrosion pits, then coalesce and grow into longer cracks. Therefore, the main cause of the decrease in the corrosion fatigue strength of the structural

steel is considered to be the appearance of the crack originating from the corrosion pit, while the increase in the load stress due to the decrease in the plate thickness caused by the general corrosion is another important factor.

3 Calculation of Long-Term Corrosion Fatigue Life

3.1 Corrosion Pit Data

A flowchart of the process for estimating the long-term corrosion fatigue life is shown in Fig. 2. Here, the calculation process was performed in the order of the flowchart.

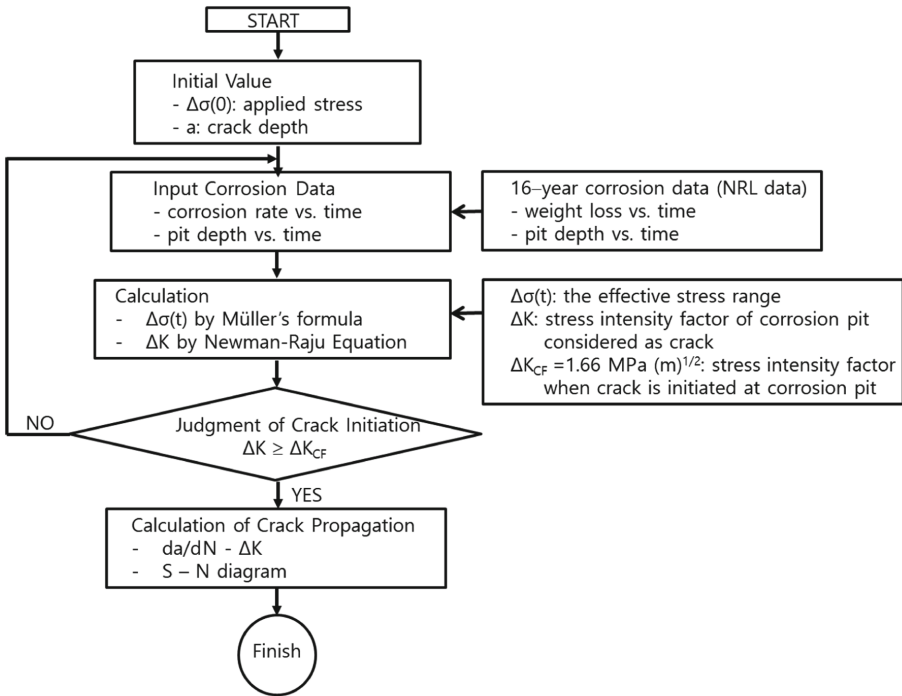


Fig. 2. Flowchart for the evaluation of long-term corrosion fatigue life.

Many studies have been conducted on the corrosion of carbon steel. Stainless steel has been known to corrode in the form of pitting corrosion. Furthermore, it is known that the corrosion of carbon steel occurs not only in the form of general corrosion, but also in the form of corrosion pits [2, 6–8]. These studies show that corrosion pits occur along with general corrosion in steel in a corrosive environment. Therefore, in this study, corrosion pits as well as general corrosion were included in the estimation of the corrosion fatigue life. This requires corrosion data for long-term general corrosion and pitting corrosion. In previous studies, corrosion data with a test duration of less than two months were found to follow a trend [6], but long-term corrosion data for long-term

corrosion fatigue life evaluation are difficult to find. Therefore, in this study, we use the results of Southwell and Alexander [9] detailing 16 years of immersion on steel as the corrosion data for the evaluation of the long-term corrosion fatigue life. Figure 3 shows the results of the weight loss and pitting penetration trends for ferrous steel.

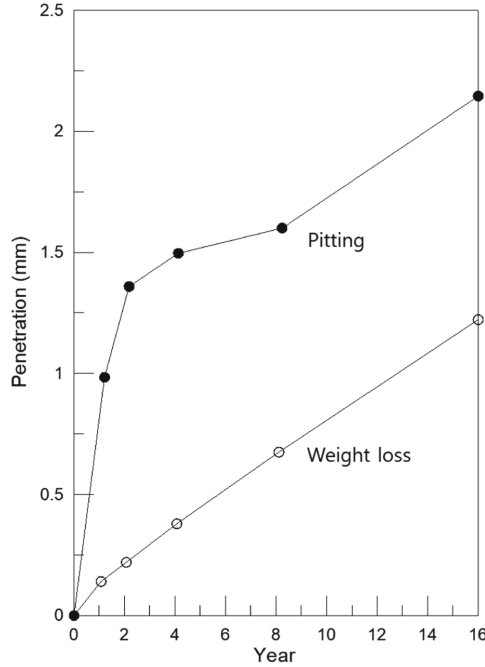


Fig. 3. Corrosion of carbon steel continuously immersed in seawater [9].

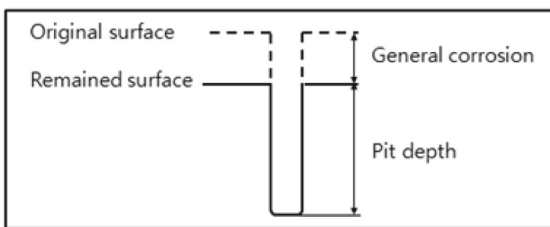


Fig. 4. Schematic of the concept of general corrosion and pitting corrosion in carbon steel.

According to Okazaki et al. [10], the regional dependence of seawater concentration is relatively small and its composition is almost the same. However, the gas components, such as dissolved oxygen, strongly depend on the temperature and water pressure, hence, caution must be paid to the evaluation of the corrosiveness.

The concept of general corrosion and pitting corrosion in this study is shown in Fig. 4. The pitting penetration represents the depth of the pit and characterizes the corrosion

pit. That is, the general corrosion by weight loss increases the applied stress, and the corrosion pit is involved in crack initiation. In this study, the corrosion values of steel were derived from the graph shown in Fig. 3. Here, the weight loss shows a nearly linear trend. Meanwhile, the pitting penetration shows a rapid increase up to approximately 2 years, but the weight loss gradient is gentle until the 8-year mark; then, a sharp weight loss tendency is observed again. This tendency affects the slope of the S-N curve of the corrosion fatigue. A computer program was developed to calculate the long-term corrosion fatigue life estimation according to the flowchart of Fig. 1. The relationship between the pit depth and time for each linear section, shown in Fig. 3, is expressed as a function in the calculation program, and the stress intensity factor (SIF) was calculated from the Newman-Raju equation by considering the pit as a crack.

3.2 General Corrosion Data

Consideration of the general corrosion was conducted as follows. The weight loss data of Fig. 2 exhibits an almost linear increase over the entire periods of 1 year, 2 years, 4 years, 8 years, and 16 years. The effective stress range equation of Müller [11], displayed as Eq. (1), indicates the increase in the applied stress range according to the reduction in the cross-sectional shape. In this study, the long-term corrosion fatigue life of more than 20 years, corresponding to the life of the ship, was evaluated such that the phenomenon of the increased stress due to general corrosion could be expressed using Eq. (1). We calculated the corrosion rate from the slope of the weight loss for the steel and used it to calculate the effective stress range of Eq. (1) due to the increase in the applied stress range from the reduction in the cross-sectional area. In this study, this was considered to be the effect of general corrosion.

$$\Delta\sigma(t_h) = \Delta\sigma_0 \left(1 - \frac{R_k \cdot t_h}{r_0} \right)^{-2} \quad (1)$$

where $\Delta\sigma(t_h)$ is the effective stress range, $\Delta\sigma_0$ is the applied stress range, R_k is the corrosion rate, t_h is time ($= N/f$, where f represents the frequency), and r_0 is the radius of the circular cross-section. Considering a wave period in the ocean, 10 cpm (cycles per minute) or 0.17 Hz was adopted for the frequency. In this equation, r_0 was set to 5 mm.

3.3 Calculation of Stress Intensity Factor of Corrosion Pit

The stress intensity factor ΔK_{CF} at the time of crack initiation in the corrosion pit was calculated using Eq. (2), of the Newman-Raju equation [12].

$$K = (\sigma_t + H\sigma_b) \cdot \sqrt{\frac{\pi a}{Q}} \cdot F(a/t, a/c, c/b, \vartheta) \quad (2)$$

where σ_t is the remote uniform tension stress, σ_b is the remote outer fiber bending stress, ϑ is the parametric angle defining the position of the point under consideration, a is the crack depth, $2c$ is the crack length, t is the plate thickness, $2b$ is the plate width for the tension and bending loads, Q is the elliptical crack shape factor, and $F(a/t, a/c, c/b, \vartheta)$ is

the boundary correction factor. This equation is valid for $0 < a/c \leq 1.0$, $0 \leq a/t \leq 0.8$, $c/b < 0.5$, $0 \leq \phi \leq \pi$. Figure 5 shows a surface crack in a finite plate.

The stress intensity factor was calculated by considering the two-dimensional shape of the corrosion pit projected in the load direction as a crack. When calculating the stress intensity factor using Eq. (2), the effective stress range of $\Delta\sigma(t)$ of Eq. (1) was used for the remote stress in Eq. (2).

The pit shape was calculated as follows. The growth of the corrosion pits can be seen to continue when the corrosion pits grow or when the growth rate of the cracks in the corrosion pits is parallel to the x -axis in the corrosion fatigue crack growth curve.

The growth of the corrosion pits is known to have a constant aspect ratio [3, 6]. Komai determined the maximum, average, and minimum aspect ratios in the corrosion pits where cracks occurred during the HT50-TMCP experiments. Here, the average aspect ratio of HT50-TMCP was 0.65. Therefore, the aspect ratio for the growth of the corrosion pits in this calculation was specified as 0.65.

3.4 Stress Intensity Factor of ΔK_{CF} at the Moment of Corrosion Fatigue Crack Initiation

Komai [6] defined the moment of the occurrence of a crack from a corrosion pit as the crack initiation life of the corrosion fatigue by using high-tensile stress steel, a kind of carbon steel. The conversion of a corrosion pit to a crack is explained as follows [6]. For the growth law of the corrosion pit, Komai obtained the change over time of a corrosion pit under the conditions of $f = 0.17$ Hz and stress ratio $R = -1$ under cyclic stress. Next, the corrosion pits with cracks at the bottom were regarded as sharp semi-elliptical surface cracks and the K_I values at the bottom of the corrosion pits were calculated using the Newman-Raju equation. Here, the aspect ratio of the corrosion pits was 0.65. From this, it was concluded that ΔK at the bottom of the corrosion pit does not necessarily increase even when the number of cycles or pit depth is increased, and that the average value ΔK_{CF} is maintained at a substantially constant value, with $\Delta K_{CF} = 1.66$ MPa (m)^{1/2}.

From this, it was reported that the mechanical condition of the pit, with the crack obtained from the fracture test, reflects that at the time of cracking, and the occurrence of the crack from the bottom of the pit is well organized by the ΔK_{CF} obtained from the pit with the crack. Therefore, in this study, the aspect ratio of the growth of pits was $a/c = 0.65$ and the average $\Delta K_{CF} = 1.66$ MPa (m)^{1/2} when considering the cracks generated from pits.

In this study, this concept was used to estimate the corrosion fatigue life of carbon steel. Komai proposed $\Delta K_{CF} = 1.66$ MPa (m)^{1/2} as the corrosion fatigue crack initiation life (N_c) of carbon steel, which was adopted in this study. Moreover, in this study, N_c was determined when the calculated stress intensity factor of the pit, considering a crack, reached $\Delta K_{CF} = 1.66$ MPa (m)^{1/2}. Table 1 shows the crack size at the time of the crack initiation and the number of cycles of crack initiation life at each applied stress.

Table 1. Calculation results of crack initiation life and crack depth.

Stress amplitude (MPa)	Number of cycles (Ni)	Crack depth (mm)
10	83,195,892	2.11
20	4,872,132	0.74
30	2,280,924	0.35
40	1,307,844	0.2
50	845,172	0.13
60	589,968	0.09
70	434,520	0.07
80	333,540	0.05
90	263,772	0.04
100	214,200	0.03
200	53,856	0.01
300	23,868	0.004

3.5 Calculation of Crack Propagation Life

The crack propagation life was calculated using the Newman-Raju equation with the fatigue crack initiation length as the initial crack length. The thickness t was set to infinity and the half-width b was set to 10 mm. When the thickness is thin, the length of the width has a great influence on the calculation result, but when the thickness is infinite, the calculation result is not changed when the half-width is compared between 10 mm and 20 mm.

$$da/dN = C(\Delta K)^m \tag{6}$$

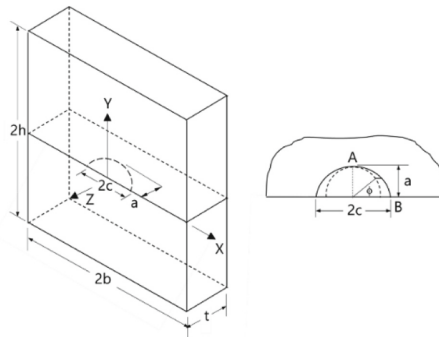


Fig. 5. Surface crack in a finite plate.

The aspect ratios in the fatigue crack growth calculations were determined using the fatigue crack growth patterns of surface cracks as presented in the appendix of the paper by Newman and Raju [12], as follows. At point A and B in the figure, the following equations can be given.

$$\frac{da}{dN} = C_A \Delta K_A^n \tag{3}$$

$$\frac{dc}{dN} = C_B \Delta K_B^n \tag{4}$$

Because the stress intensity factor solution for the small semicircular crack shows that the stress intensity at point B is approximately 10% higher than that at point A, the coefficient C_B was assumed to be:

$$C_B = 0.9^n C_A \tag{5}$$

Therefore, in this paper, additional crack growth calculations were carried out. The crack propagation life was calculated using the Paris equation, shown in Eq. (2). The relationship between the SIF and the crack propagation rate is shown in Fig. 6.

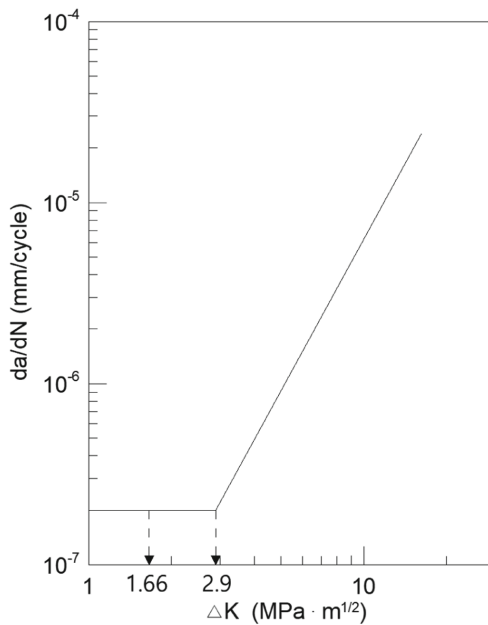


Fig. 6. Relationship between stress intensity factor ΔK and da/dN [13].

The crack propagation characteristics used in the crack propagation calculation were adopted from the da/dN - ΔK curve for the HT50-TMCP proposed by Komai et al. [13]. Komai et al. proposed the following for the crack propagation life evaluation. That is, in

the case of small cracks, there is no crack closure phenomenon in corrosion fatigue crack growth. From this, it is possible to use the propagation characteristics of the long crack obtained by avoiding the occurrence of crack closure under the condition of constant K_{max} when the propagation characteristics of a small crack cannot be obtained.

Table 2. Calculation results of crack propagation life and fracture life.

Stress amplitude (MPa)	Number of cycles at $\Delta K = 2.9 \text{ MPa}\cdot(\text{m})^{1/2}$	Number of cycles (Nf) from $\Delta K = 2.9 \text{ MPa}\cdot(\text{m})^{1/2}$ until fracture ($t = 9.99 \text{ mm}$)
10	99,719,892	117,785,609
20	12,851,388	31,179,436
30	5,601,636	17,130,798
40	3,292,560	11,123,643
50	2,153,016	7,750,287
60	1,476,756	5,620,265
70	1,119,960	4,315,199
80	861,696	3,406,142
90	682,992	2,747,496
100	554,472	2,269,758
200	139,536	631,976
300	62,118	293,951

Table 3. Summary of the evaluation methods.

	Crack initiation (Ni)	Crack propagation (Np)	
		Parallel part of da/dN- ΔK curve (Fig. 5)	Slope part of da/dN- ΔK curve (Fig. 5)
Calculation	Calculation of ΔK until $\Delta K = 1.66 \text{ MPa}\cdot(\text{m})^{1/2}$	Calculation of crack propagation life from $\Delta K=1.66 \text{ MPa}\cdot(\text{m})^{1/2}$ until $\Delta K=2.9 \text{ MPa}\cdot(\text{m})^{1/2}$	Calculation of crack propagation life from $\Delta K=2.9 \text{ MPa}\cdot(\text{m})^{1/2}$ until fracture($t=9.99\text{mm}$)
Stress Intensity Factor K_I formula	Newman-Raju Equation		
Aspect ratio (a/c)	a/c = 0.65	a/c = 0.65	$C_B = 0.9^n \cdot C_A$, See 3.5
Stress range	$\Delta\sigma(t_h) = 2 \cdot \sigma_a \cdot \sigma_r$; stress amplitude, stress ratio R = -1		
Weight loss	Considered. $\Delta\sigma(t_h) = \Delta\sigma_0 \left(1 - \frac{R_k \cdot t_h}{r_0}\right)^{-2}$ is used for the calculation.	Considered. $\Delta\sigma(t_h) = \Delta\sigma_0 \left(1 - \frac{R_k \cdot t_h}{r_0}\right)^{-2}$ is used for the calculation.	<u>Not included yet.</u> $\Delta\sigma(t_h) = \Delta\sigma_0 \left(1 - \frac{R_k \cdot t_h}{r_0}\right)^{-2}$ at $\Delta K=2.9 \text{ MPa}\cdot(\text{m})^{1/2}$ is used for the calculation.
Pitting corrosion	Pit depth is used as a crack depth at Newman-Raju equation.		
Frequency	10 cycles per minute, 0.17Hz		

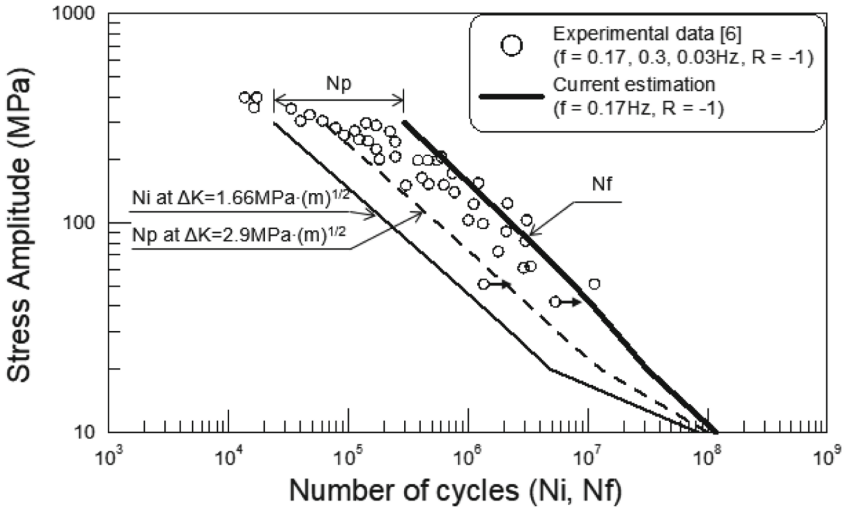


Fig. 7. Detailed description of calculation result.

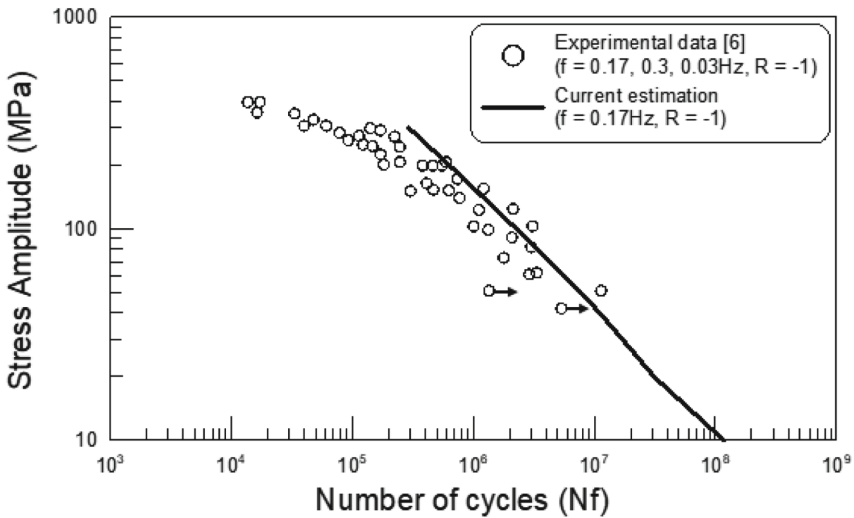


Fig. 8. Comparison between the calculation result from the current research and the experimental results from the literature [6].

For the crack closure, ΔK_{eff} was measured and considered as $\Delta K_{eff} = \Delta K$, it is possible to evaluate the crack propagation life, including the case where the crack size is small, using long crack data. The crack propagation curves for HT50-TMCP thus obtained were used to calculate the crack propagation life of this study. This was then used for comparison with the corrosion fatigue test results by HT50-TMCP on the S-N curve. In this diagram, from the Paris equations at the slope line, $c = 1.0339 \times 10^{-8}$ and

$m = 2.7824$. The results of the crack propagation life calculation are shown in Table 2. Table 3 shows summary of the evaluation methods.

The weight loss effect in the integration calculation of the slope section of the Paris equation of Fig. 5 is not yet included in the calculation results. If the effect of weight loss in this interval is included in the results, the Nf (Life to Failure) will go further to the left. Figure 7 shows detailed description of calculation results. Figure 8 shows a comparison of the calculation results of the stress amplitude in the above calculation with the corrosion fatigue test results of carbon steel obtained in [6]. The results of the calculations are in good agreement with the experimental results in the low-stress region, and the consideration of the general corrosion and pitting corrosion reflects the experimental results well.

4 Conclusion

In this study, the long-term corrosion fatigue life was estimated by considering the effect of general corrosion and pitting corrosion using the weight loss and pit corrosion information obtained from 16 years long-term corrosion data of carbon steel. The calculation of the corrosion fatigue life was performed under the same conditions as that of the corrosion fatigue strength for comparison of the calculated results with the results of the long-term S-N test conducted under the corrosive environment, with the stress ratio $R = -1$ and the load frequency $f = 0.17$ Hz. From the above calculation results, the applicability of the corrosion fatigue strength evaluation method, considering not only pit corrosion but also weight loss by using long-term corrosion data, was examined in the evaluation of the corrosion fatigue strength.

References

1. Jaske, C.E., Payer, J.H., Balint, V.S.: Corrosion Fatigue of Metals in Marine Environments. Springer-Verlag, New York Heidelberg Berlin, Battelle-Press, Columbus Ohio (1981)
2. Nagai, K., Mori, M., Yajima, H., Yamamoto, Y., Fujimoto, Y.: Studies on the evaluation of corrosion fatigue crack initiation life in notched mild steel plate. Soc. Naval Archit. Jpn. **142**, 239–250 (1977)
3. Kondo, Y.: Prediction method of corrosion fatigue crack initiation life based on corrosion pit growth mechanism. Trans. Japanese Soc. Mech. Eng. (A) **53**(495), 1983–1987 (1987)
4. Lindley, T.C., McIntyre, P., Trant, P.J.: Fatigue-crack initiation at corrosion pits. Metals Technol. **9**(135) (1982)
5. Kim, W.B., Paik, J.K., Yajima, H.: Evaluation of corrosion fatigue crack initiation life of 13Cr steel. Key Eng. Mater. **326**, 1007–1010 (2006)
6. Komai, K.: Environmental Strength Design of Structural Materials, 1st edn. Youkendou, Tokyo (1993). (in Japanese)
7. Kim, W.B., Paik, J.K., Iwata, M., Yajima, H.: Fatigue strength of rusting decayed hull steel plate in air and artificial seawater condition. J. Soc. Naval Archit. Korea **40**(1), 63–68 (2006)
8. Funatsu, Y.: Building better oil tankers. ClassNK Magazine, pp. 11–14 (2009)
9. Southwell, C.R., Alexander, A.I.: Corrosion of metals in tropical environments, Part 9 – Structural ferrous metals – Sixteen years' exposure to sea and fresh water. NRL Report 6862, Naval Research Laboratory, Washington, D.C. (1969)

10. Ozaki, T., Ishikawa, Y., Akiyama, M.: Corrosion of seawater equipment – damage and countermeasures, 2nd edn. Kagakutoshoshuppan, Tokyo (2007). (in Japanese)
11. Müller, M.: Theoretical considerations on corrosion fatigue crack initiation. *Metall. Trans. A* **13A**, 649–655 (1982)
12. Newman, J.C., Raju, I.S.: An empirical stress-intensity factor equation for the surface crack. *Eng. Fract. Mech.* **15**(1–2), 185–192 (1981)
13. Komai, K., Minoshima, K., Kim, G.S.: An estimation method of long-term corrosion fatigue growth characteristics. *Trans. Japanese Soc. Mech. Eng. (A)* **54**(499), 509–512 (1987)